Electronic Supplementary information - Photostabilisation of an omniphobic, drop-castable surface coating by transformation of a self-assembled supramolecular xerogel into a covalent polymer xerogel

Janos Wasternack,[a] Tom White,[a] Sebastian Müller[a] and Christoph A. Schalley*,[a]

a Institut für Chemie und Biochemie, Freie Universität Berlin, Arnimallee 22, 14195 Berlin, Germany

* Correspondence: c.schalley@fu-berlin.de

Table of Contents

Section S1: General methods

^{1}H and ^{13}C NMR experiments were performed on JEOL ECX 400, ECP 500 and ECZ 600 and on Bruker AVANCE 500 instruments. Residual solvent signals were used as the internal standards. All shifts are reported in ppm and NMR multiplicities are abbreviated as s (singlet), d (doublet), t (triplet), m (multiplet) and b (broad).

High-resolution ESI mass spectra were recorded on an Agilent 6210 ESI-TOF mass spectrometer. HPLC grade solvents were used for sample preparation and the samples introduced into the ion source with a flow rate of 2-4 µL/min.

FTIR spectra were measured on an FTIR-ATR Nicolet iS10 Smart DuraSamplIR device.

Scanning electron microscopy (SEM) measurements were done on a scanning electron microscope from Hitachi (SU 8030). Samples were sputtered with a 5 nm gold layer using the sputtering system SC 500 from Emscope.

Section S2: Synthetic Procedures

All reagents and solvents were obtained from commercial sources and used without further purification. Perfluorohexyl ethyl iodide was purchased from abcr and used without further purification. Dry solvents were purchased from Acros Organics. Deuterated solvents were purchased from Eurisotop. Menzel™ glass cover slides (22 mm × 22 mm × 0.13-0.16 mm) were purchased from VWR.

Thin-layer chromatography was performed on silica-gel-coated plates with fluorescent indicator F254 (Macherey-Nagel). For column chromatography, silica gel (0.04-0.063 mm, Macherey-Nagel) was used.

4-Hydroxy-N-(prop-2-yn-1-yl)butanamide (alcohol **3**)

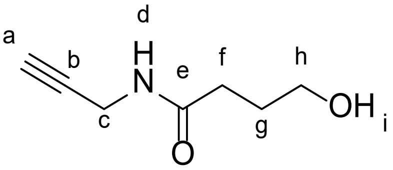

According to a literature procedure[S1], a neat mixture of γ-butyrolactone (10.0 ml, 131 mmol, 1.0 equiv.) and propargylamine (13.0 mL, 203 mmol, 1.5 equiv.) was heated to 125 °C for 3 h. The workup was adapted from a literature procedure[S2] for the synthesis of the allyl analogue of substance **3**: After cooling to rt, the brown residue was transferred with dichloromethane into a 50 ml Kugelrohr bulb, the solvent was removed and the residue subjected to Kugelrohr distillation. Excess propargylamine was removed at 65 °C, 0.5 mbar during the first 10 min, then the reaction mixture was heated to 105°C, 0.01 mbar for 10 min to remove traces of γ-butyrolactone. The product distilled between 150 - 180 °C at 0.01 mbar.

Product **3** was obtained as a light-yellow oil that solidified within an hour (16.0 g, 11.3 mmol, 87% yield). The NMR data of the isolated substance are in agreement with the literature[S1].

^{1}H NMR (600 MHz, $CDCl_3$, ppm): δ = 6.78 (b: 1H, N*H*, d), 4.00 (dd: 2H, C*H*$_2$, c), 3.65 (t: 2H, C*H*$_2$, h), 3.65 (b: 1H, O*H*, i), 2.35 (t: 2H, C*H*$_2$, f), 2.23 (t: 1H, CC*H*, a), 1.85 (tt: 2H, C*H*$_2$, g).

$^{13}C\{^1H\}$ NMR (125 MHz, $CDCl_3$, ppm): δ = 173.6 (e), 79.7 (b), 71.6 (a), 62.0 (h), 32.0 (c), 29.3 (f), 28.1 (g).

HRMS (ESI): m/z calculated for $C_7H_{12}NO_2$ $[M+H]^+$ 142.0863, found 142.0862.

N,N'-(Hexa-2,4-diyne-1,6-diyl)bis(4-hydroxybutanamide) (diacetylene **2**)[S3,S4]

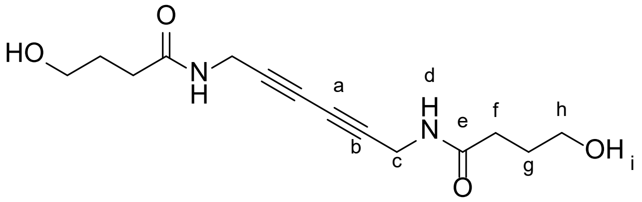

Alcohol **3** (1.36 g, 9.6 mmol, 1.0 equiv.) was dissolved in acetone (200 mL). CuCl (200 mg, 2.00 mmol, 0.2 equiv.) and TMEDA (230 mg, 1.94 mmol, 0.2 equiv.) were added. The mixture was stirred and purged with air for 2 d. The solid residue was suspended in acetone (50 mL) by sonication for 20 min. The resulting slurry was filtered yielding a first crop of product (250 mg). Slow evaporation of the green mother liquor yielded a second batch of larger crystals (900 mg).

Diacetylene **2** was obtained as a colourless solid, that becomes intensely violet within a few months of storing at 4°C as well as in contact with UV light (1.15 g, 4.01 mmol, 85% yield).

^1H NMR (600 MHz, DMSO-*d*$_6$, ppm): δ = 8.30 (t: 2H, N*H*, d), 4.47 (t: 2H, O*H*, i), 3.95 (d: 4H, C*H*$_2$, c), 3.34 (t: 4H, C*H*$_2$, h), 2.11 (t: 4H, C*H*$_2$, f), 1.62 (tt: 4H, C*H*$_2$, g).

$^{13}C\{^1H\}$ NMR (150 MHz, DMSO-*d*$_6$, ppm): δ = 172.1 (e), 76.3 (b), 65.7 (a), 60.1 (h), 31.7 (f), 28.4 (g), 28.4 (c).

HRMS (ESI): m/z calculated for $C_{14}H_{20}N_2O_4$ $[M+H]^+$ 281.1501, found 281.1541.

Dimethyl 2-(3,3,4,4,5,5,6,6,7,7,8,8,8-tridecafluorooctyl)malonate (malonic ester **6**)

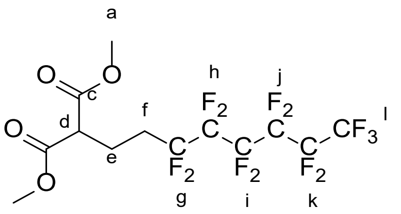

According to a literature procedure[S5], dimethyl malonate (8.75 g, 7.60 mL, 66.67 mmol, 2.0 equiv.), 2-(perfluorohexyl)ethyl iodide (15.80 g, 8.30 mL, 33.33 mmol, 1.0 equiv.), anhydrous K_2CO_3 (18.43 g, 133.33 mmol, 4.0 equiv.), 18-crown-6 (0.71 g, 2.67 mmol, 0.08 equiv.) and anhydrous tetrahydrofuran (20 mL) are mixed in a 100 mL pressure tube and purged with N_2 for 15 min. The mixture was heated to 80°C over night under an N_2 atmosphere with strong magnetic stirring. The mixture was transferred into a round bottom flask and the solvent evaporated under reduced pressure. Water (25 mL) was added, and the mixture was extracted with diethyl ether (65 mL, 2x). The organic phase was washed with hydrochloric acid (10%, 7 mL), then washed with water. After drying with Na_2SO_4 and evaporating the solvent under reduced pressure, an oil was obtained which was purified by Kugelrohr distillation. To remove excess dimethyl malonate the oil was held at 65°C, 2.7 mbar for 20 min. The residue was first cooled to room temperature and then heated slowly at a pressure of 0.01 – 0.1 mbar. The first fraction was collected up to 100°C and contained some dimethyl malonate. The second fraction was pure product and was collected from 100°C – 135°C.

Malonic ester **6** was obtained as colourless oil (7.93 g, 13.71 mmol, 41% yield, in another run 71% yield were obtained), the analytic data were consistent with the literature[S5].

^{1}H NMR (600 MHz, CDCl$_3$, ppm): δ = 3.77 (s: 6H, CH_3, a), 3.46 (t: 1H, CH, d), 2.20 (m: 4H, CH_2, e&f).

^{13}C{^{1}H} NMR (150 MHz, CDCl$_3$, ppm): δ = 169.0 (c), 52.9 (a), 50.5 (d), 28.6 (t: f), 20.0 (t: e).

^{19}F NMR (565 MHz, CDCl$_3$, ppm): δ = −80.73 (t: 3F, CF_3, l), −114.38 (m: 2F, CF_2, g), −121.81 (m: 2F, CF_2, h), −122.77 (m: 2F, CF_2, i), −123.30 (m: 2F, CF_2, j), −126.04 (m: 2F, CF_2, k).

2-(3,3,4,4,5,5,6,6,7,7,8,8,8-tridecafluorooctyl)malonic acid (malonic acid **5**)

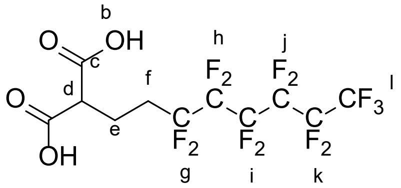

According to literature procedures[S5,S6] in a 100 mL pressure tube, KOH (85%, 5.10 g, 77.27 mmol, 5.7 equiv.) was dissolved in methanol (85 mL). Malonic ester **6** (7.90 g, 13.66 mmol, 1.0 equiv.) was added and the mixture was heated to 90 °C for 20 h with strong magnetic stirring. The mixture was transferred into a 250 mL round bottom flask and the solvent was evaporated under reduced pressure. Diethyl ether (150 mL) was added and hydrochloric acid (37%, 100 mL) was slowly added with strong stirring. After complete addition, the mixture was stirred at room temperature for 1 h. Enough water and diethyl ether were added to completely dissolve all the solids and the phases were separated. The aqueous phase was extracted with diethyl ether (200 mL, 2x), then the combined organic phases were washed with water (135 mL, 2x), dried with Na$_2$SO$_4$ and the solvent was evaporated under reduced pressure.

Malonic acid **5** was obtained as a colourless, crystalline solid (7.25 g, 16.10 mmol, 98% yield), the analytic data were consistent with the literature[S5,S6].

^{1}H NMR (600 MHz, acetone-d_6, ppm): δ = 3.61 (t: 1H, CH, d), 2.42 (tt: 2H, CH2, f), 2.19 (dt: 2H, CH2, e).

^{13}C{^{1}H} NMR (150 MHz, acetone-d_6, ppm): δ = 170.3 (c), 50.6 (d), 29.1 (t: f), 20.6 (t: e).

^{19}F NMR (565 MHz, acetone-d_6, ppm): δ = −81.61 (t: 3F, CF_3, l), −115.00 (m: 2F, CF_2, g), −122.37 (m: 2F, CF_2, h), −123.34 (m: 2F, CF_2, i), −123.98 (m: 2F, CF_2, j), −126.67 (m: 2F, CF_2, k).

5,5,6,6,7,7,8,8,9,9,10,10,10-tridecafluorodecanoic acid (fluorous acid **4**)

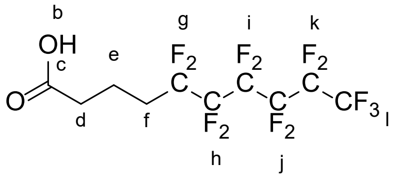

According to literature procedures[S5,S6] neat malonic acid **5** (7.50 g, 16.70 mmol, 1.0 equiv.) in a 25 mL round bottom flask was lowered into a preheated woods metal bath at a temperature of 195°C and was kept at this temperature for 0.5 h until gas evolution ceased (observable by an attached silicone oil bubbler). The melt was cooled to approximately 150°C, toluene (5 mL) was carefully added ensuring complete dissolution. The solution was slowly cooled to rt and the crystalline solid was filtered and washed with room temperature *n*-pentane (5 mL). The solid was air dried, because drying under vacuum lead to significant losses of the quite volatile product. An additional impure fraction can be obtained from the mother liquor (0.6 g).

Fluorous acid **4** was obtained as 2-4 cm long, colourless needles (5.75 g, 14.15 mmol, 85% yield), the analytic data were consistent with the literature[S5,S6].

^{1}H NMR (600 MHz, $CDCl_3$, ppm): δ = 2.50 (t: 2H, C*H*, d), 2.17 (tt: 2H, C*H*$_2$, f), 1.97 (tt: 2H, C*H*$_2$, e).

^{13}C{^{1}H} NMR (150 MHz, $CDCl_3$, ppm): δ = 178.3 (c), 32.9 (d), 30.2 (t: f), 15.8 (e).

^{19}F NMR (565 MHz, $CDCl_3$, ppm): δ = −80.77 (t: 3F, C*F*$_3$, l), −114.42 (m: 2F, C*F*$_2$, g), −121.87 (m: 2F, C*F*$_2$, h), −122.83 (m: 2F, C*F*$_2$, i), −123.46 (m: 2F, C*F*$_2$, j), −126.11 (m: 2F, C*F*$_2$, k).

HRMS (ESI): m/z calculated for $C_{38}H_{30}F_{34}N_2O_6$ [M+K]$^+$ 405.0160, found 405.0195.

FTIR: ν_{as} C=O 1698 cm^{-1}.

(Hexa-2,4-diyne-1,6-diylbis(azanediyl))bis(4-oxobutane-4,1-diyl) bis(5,5,6,6,7,7,8,8,9,9,10,10,10-tridecafluorodecanoate) (diacetylene **1**)

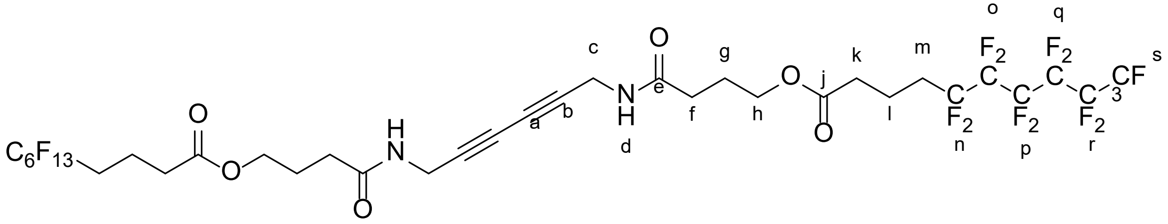

In a 100 mL pressure tube, fluorous acid **4** (1.77 g, 4.36 mmol, 2.2 equiv.) was dissolved in anhydrous THF (50 mL) and the mixture purged with N_2 for 2 min. EDC·HCl (1.14 g, 5.94 mmol, 3.0 equiv.) was added and the mixture was stirred at rt for 30 min to form the activated carboxylic acid reagent. Diacetylene **2** (0.555 g, 1.98 mmol, 1.0 equiv.) and 4-(dimethylamino)pyridine (0.85 g, 6.93 mmol, 3.5 equiv.) were added and the light-purple suspension was stirred at rt for 90 min under N_2, and then heated to 70 °C in the closed pressure tube for 30 min under exclusion of light.

The solvent was evaporated under reduced pressure and the residue was purified by flash column chromatography, eluting with DCM → 10% acetone in DCM → 20% acetone in DCM.

Diacetylene **1** was obtained as colourless solid (1.21 g, 1.15 mmol, 58% yield), that becomes pink due to partial thermal polymerisation within a few weeks of storing at 4°C. In contact with UV light the product polymerises quickly into a cherry red polydiacetylene, which is insoluble in chloroform.

^{1}H NMR (500 MHz, $CDCl_3$, ppm): δ = 5.84 (b: 2H, N*H*, d), 4.15 (t: 4H, C*H*$_2$, h), 4.12 (d: 4H, C*H*$_2$, c), 2.43 (t: 4H, C*H*$_2$, k), 2.27 (t: 4H, C*H*$_2$, f), 2.16 (tt: 4H, C*H*$_2$, m), 2.01 (tt: 4H, C*H*$_2$, g), 1.95 (tt: 4H, C*H*$_2$, l).

^{13}C{^{1}H} NMR (125 MHz, $CDCl_3$, ppm): δ = 172.6 (e), 171.6 (j), 74.3 (b), 67.4 (a), 63.9 (h), 33.1 (k), 32.7 (f), 30.2 (m), 29.9 (c), 24.6 (g), 16.0 (l).

^{19}F NMR (471 MHz, $CDCl_3$, ppm): δ = −80.68 (t: 6F, C*F*$_3$, s), −114.30 (m: 4F, C*F*$_2$, n), −121.81 (m: 4F, C*F*$_2$, o), −122.77 (m: 4F, C*F*$_2$, q), −123.40 (m: 4F, C*F*$_2$, p), −126.03 (m: 4F, C*F*$_2$, r).

HRMS (ESI): m/z calculated for $C_{34}H_{30}F_{26}N_2O_6$ $[M+Na]^+$ 1079.1586, found 1079.1419.

Section S3: NMR Spectra

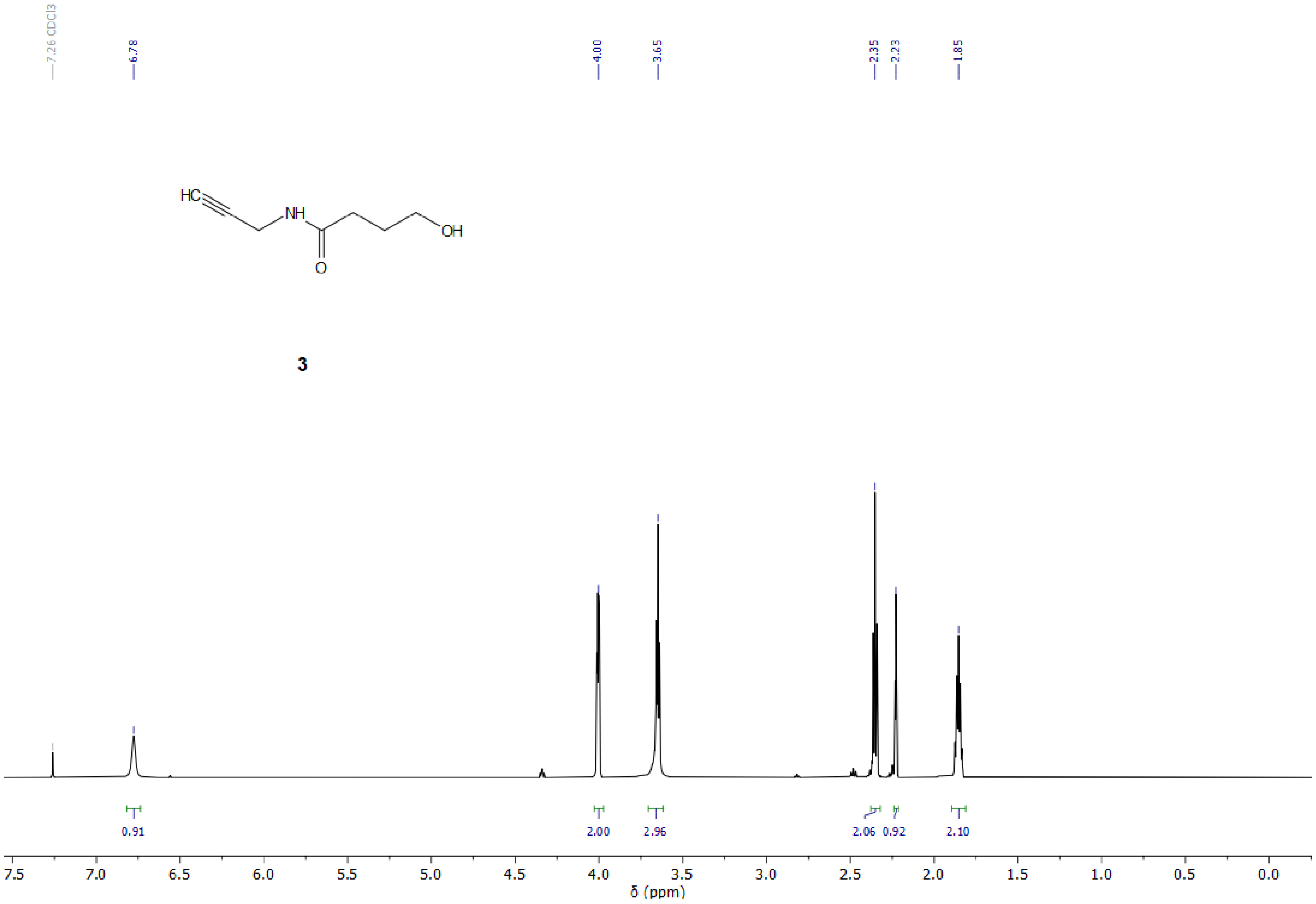

*Spectrum 1: ^{1}H NMR-spectrum of alcohol **3**, 600 MHz, CDCl$_3$, 20°C.*

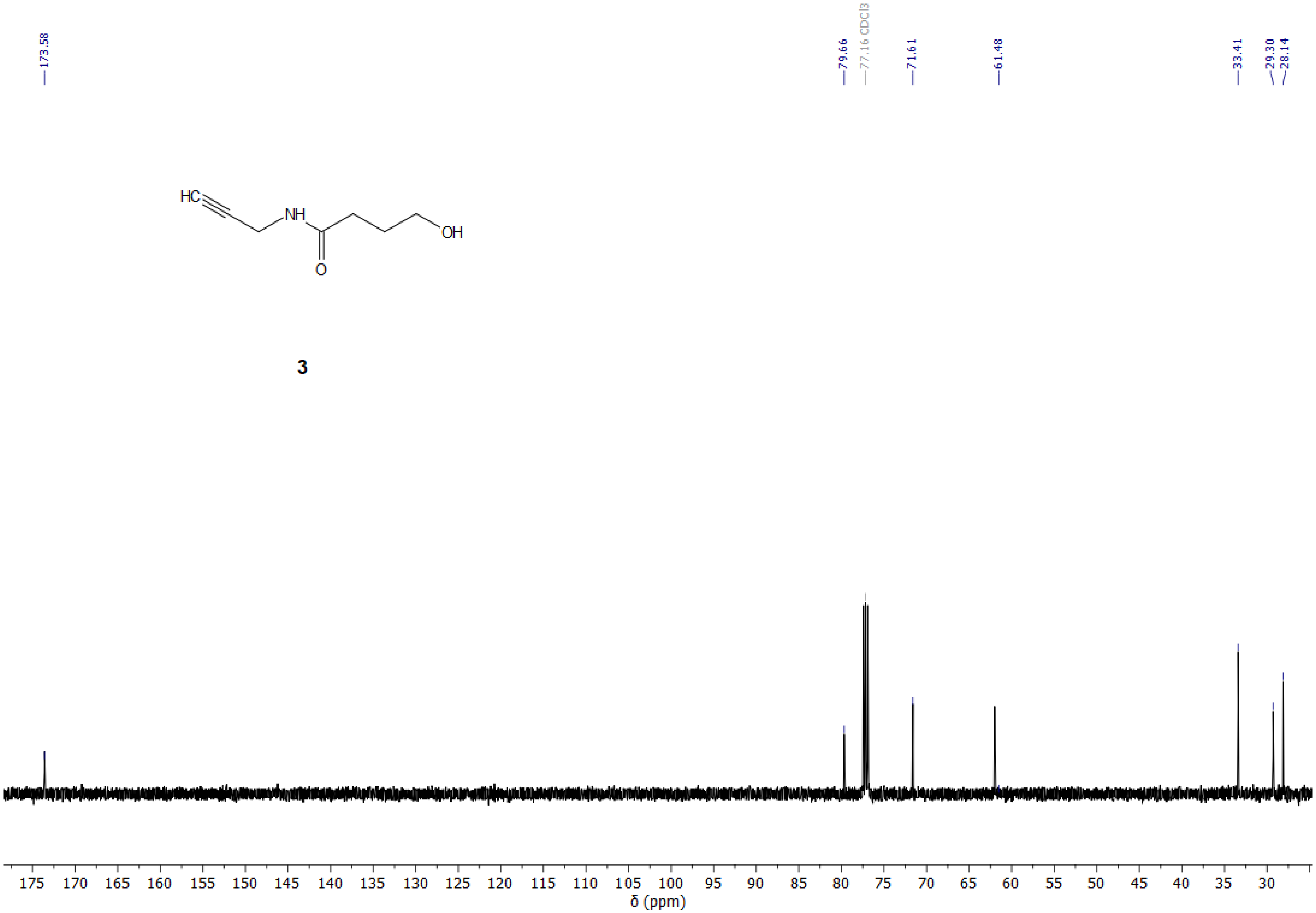

*Spectrum 2: $^{13}C\{^{1}H\}$ NMR-spectrum of alcohol **3**, 125 MHz, $CDCl_3$, 20°C.*

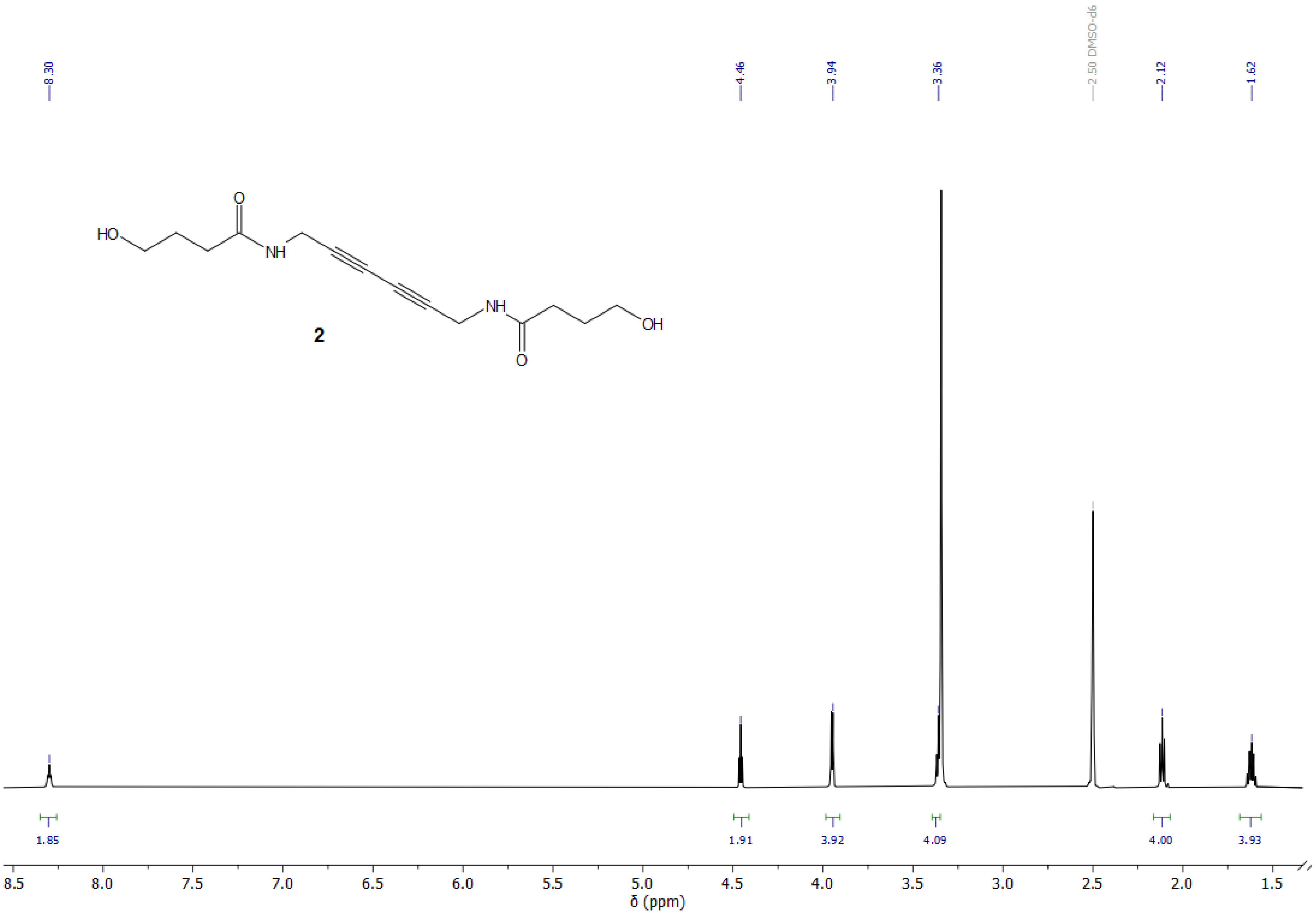

Spectrum 3: ^{1}H NMR-spectrum of diacetylene ***2****, 600 MHz, DMSO-d_6, 20°C.*

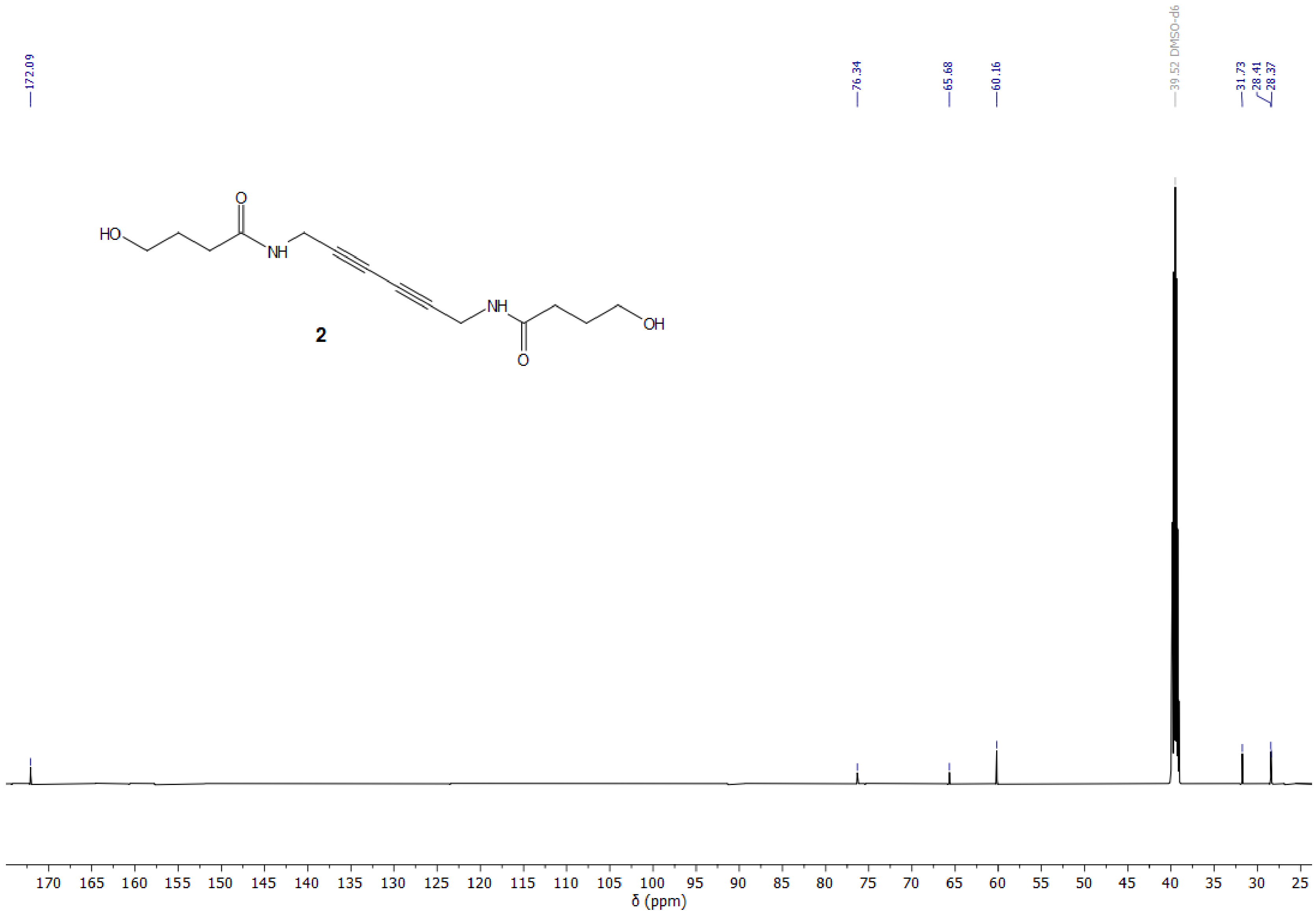

*Spectrum 4: ^{13}C{^{1}H} NMR-spectrum of diacetylene **2**, 125 MHz, DMSO-d_6, 20°C.*

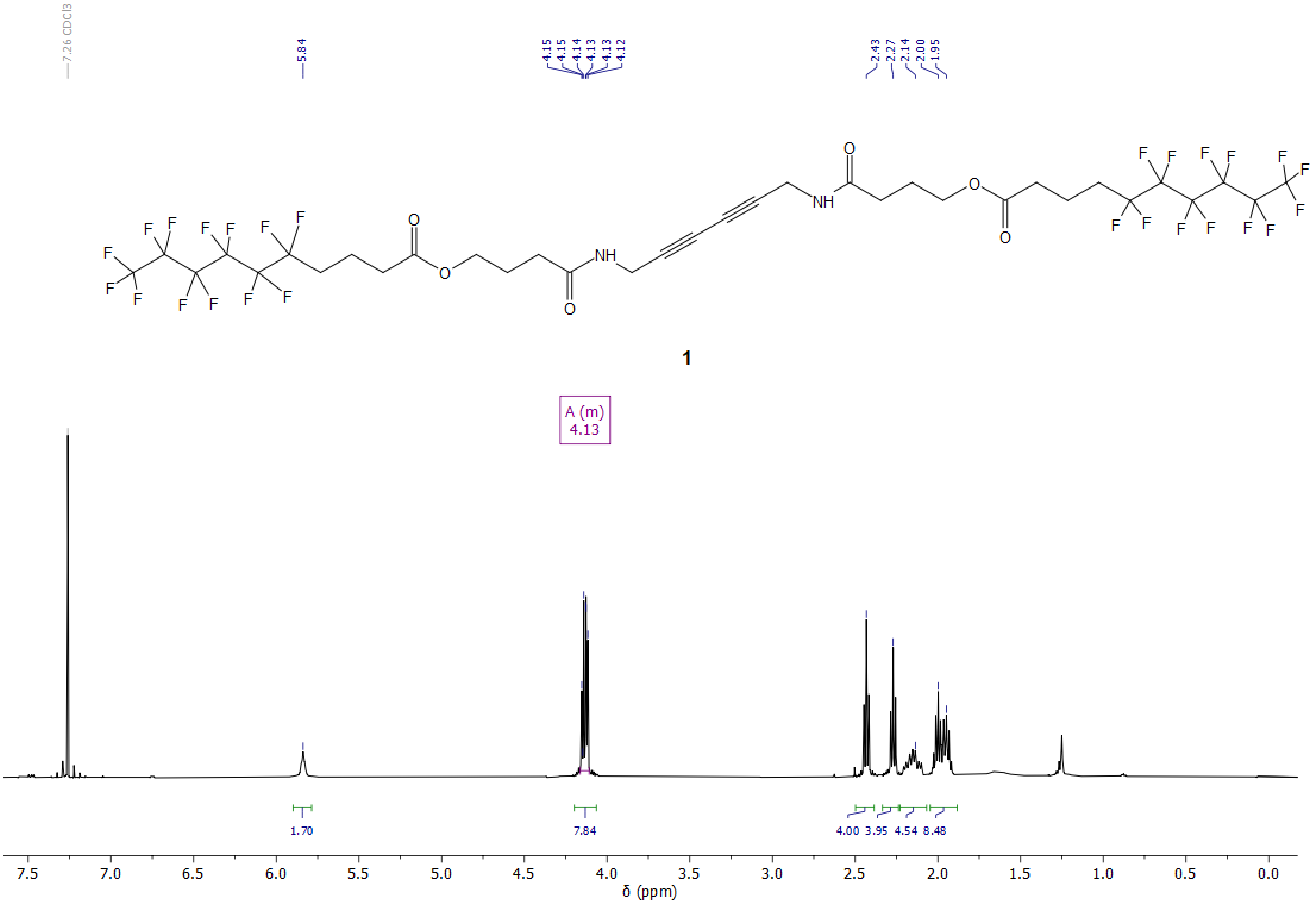

*Spectrum 5: ^{1}H NMR-spectrum of diacetylene **1**, 600 MHz, $CDCl_3$, 20°C.*

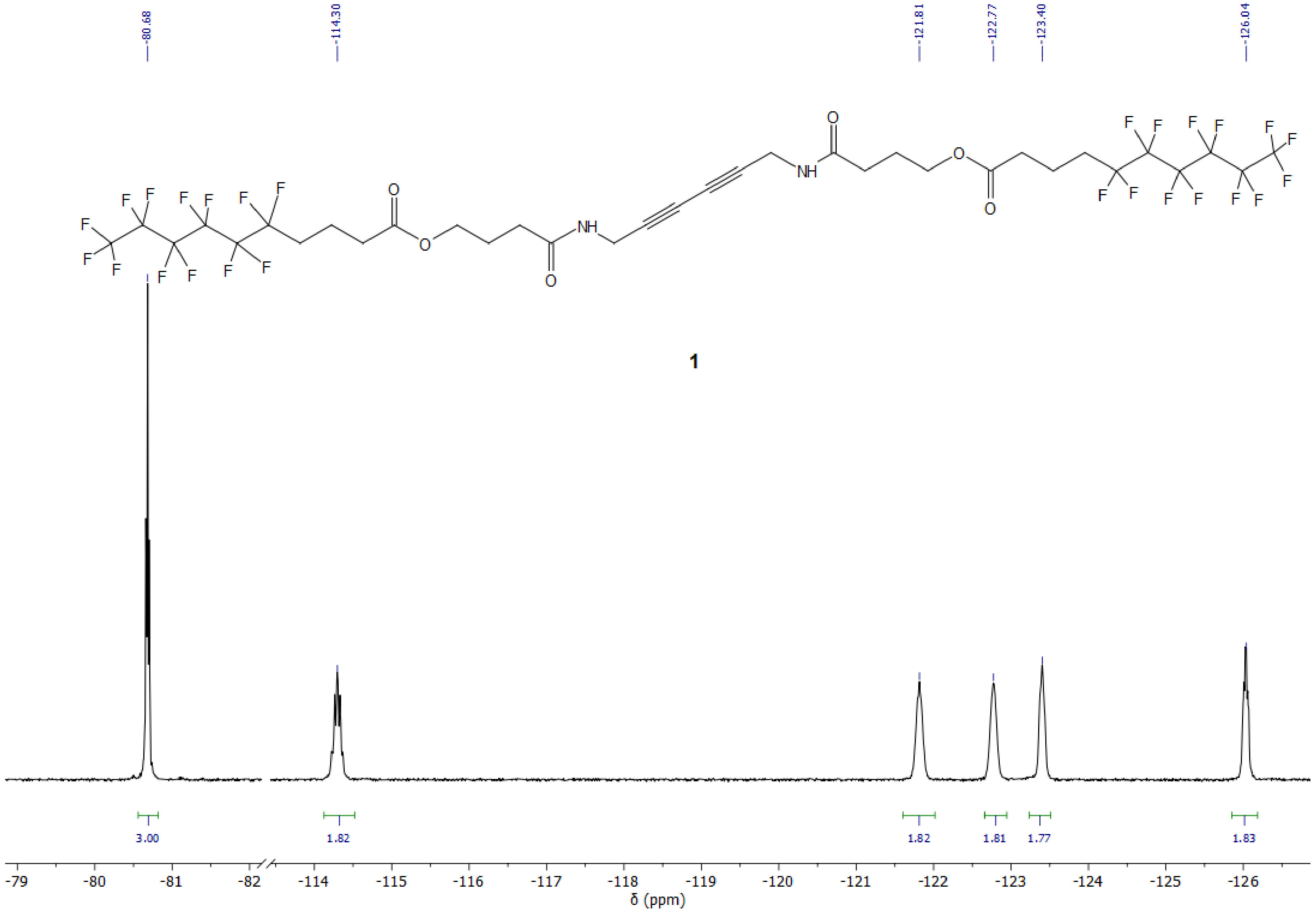

1

*Spectrum 6: ^{19}F NMR-spectrum of diacetylene **1**, 471 MHz, CDCl$_3$, 20°C.*

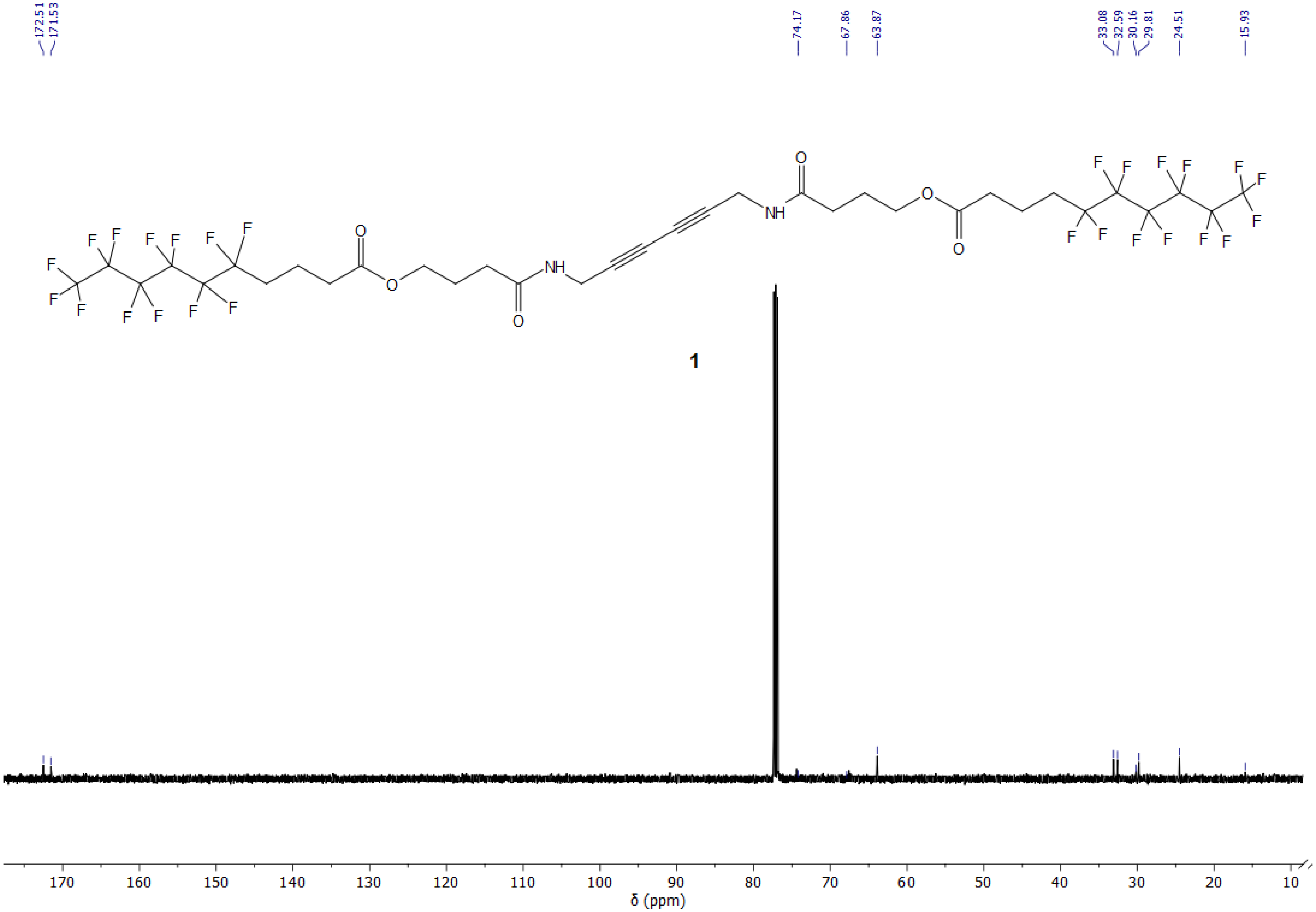

Spectrum 7: ^{13}C{^{1}H} NMR-spectrum of diacetylene ***1****, 125 MHz, CDCl$_3$, 20°C.*

Section S4: Drop casting procedure

Figure S1: Setup for drop casting in environments of controlled RH.

LMWG **1** (25 mg) was added to chloroform (1.5 ml or 2.0 ml for dilute solutions) and homogenised by sonication for 1.5 min.

Drop-casting was performed within 'humidity boxes' at 21°C, setup as seen in Figure S1. The relative humidity within the boxes was maintained at a constant level of 99% using distilled water, 82 ± 1 % with saturated potassium chloride solution, and 72 ± 1% with saturated sodium chloride solution.[S7] Faster equilibration to the desired relative humidity was achieved by placing a filter paper cone in the salt solution to increase the surface area. Menzel-Glaser microscope glass coverslips (22 × 22 mm) were cleaned by immersion in piranha solution (H_2SO_4 (96%) / H_2O_2(30%) 3/1 V/V) and subsequent rinsing with distilled water and acetone. Four slides were placed on level surfaces within the boxes. The freshly prepared sol of LMWG **1** (0.3 ml) was carefully added to the slides ensuring complete coverage by the liquid. The boxes were left in an undisturbed place for drying (0.5 h). After opening the boxes to take out the samples, the desired relative humidity reached equilibrium again after a few hours. Native coatings were characterised on the day of their preparation to avoid polymerisation due to ambient light and thermally induced polymerisation.

Section S5: Irradiation procedure

Polymerised surfaces were prepared by irradiating the coating in a UV exposure chamber (Beltron UV- Box 850 S) with a standard mercury UVH-lamp. The coatings were placed on an aluminium block (4 cm x 2 cm x 4 cm) that was precooled by liquid nitrogen. The coating was then irradiated at 100 % power mode for 1 minute.

Section S6: UV/Vis spectra

UV/Vis spectra were recorded with a Varian Cary 50 Bio spectrometer equipped with a xenon lamp. HPLC grade solvents were used. A representative sample for UV/Vis spectroscopy was prepared by depositing the coating on the inside of a cuvette. A solution of LMWG **1** (3.4 mg) in chloroform (0.2 mL) was dropcast onto one internal side of a 1 mm path length Suprasil cuvette and left to dry at ambient conditions. A UV/Vis spectrum of the dried native film was recorded. The cuvette was then irradiated before recording the spectrum of the polymerised material.

Section S7: Morphology analysis

Optical microscope images were taken with a Zeiss Microscope Axio Scope.A1 MAT with dark-field microscopy, an Axiocam 105 colour camera and the Zeiss ZEN core v.2.7 software. Some of the images were taken with the extended depth of focus function in the software, which stacks layers of images, creating an image with focus on different heights (EDF). The panorama function of the software was used to view an entire scratch stretching the length of the coating. Additionally, mean pore diameters were calculated using the measuring tool function. Fifteen pores were selected within a given area of the coating selecting those which are representative of the mean pore size according to their abundance seen in the micrograph.

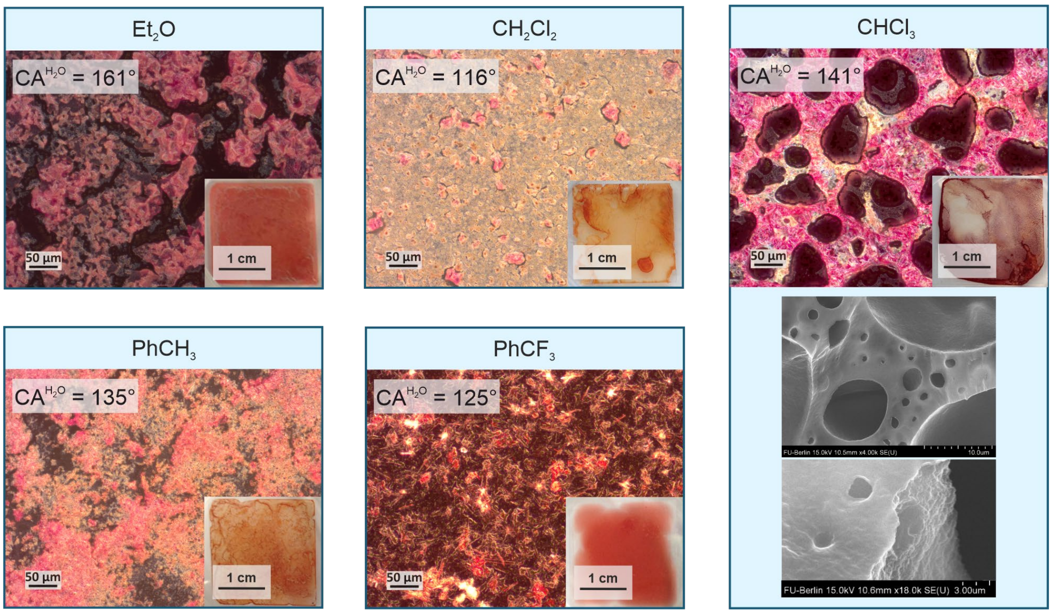

Figure S2: Morphology of coatings obtained from different solvents.

Section S8: Omniphobicity

Contact angles were determined on a Dataphysics Contact Angle System (OCA 20) and images were analysed with the automatic contact angle measuring and contour analysis system with the LAPLACE YOUNG equation using the software SCA 20 U. Contact angles are the mean value of three independent measurements with a drop volume of 3 µL on different locations on one surface. The average of 15 independent measurements across 3 different surfaces, prepared under the same conditions. Milli-Q water was used to determine hydrophobicity and *n*-decane was used to determine oleophobicity. To determine the aqueous wetting behaviour of the coatings, the surfaces were tilted, resulting in adhesion of the droplets even at 180°. A broken coating was examined from its side by light microscopy to determine the pore structure in vertical orientation.

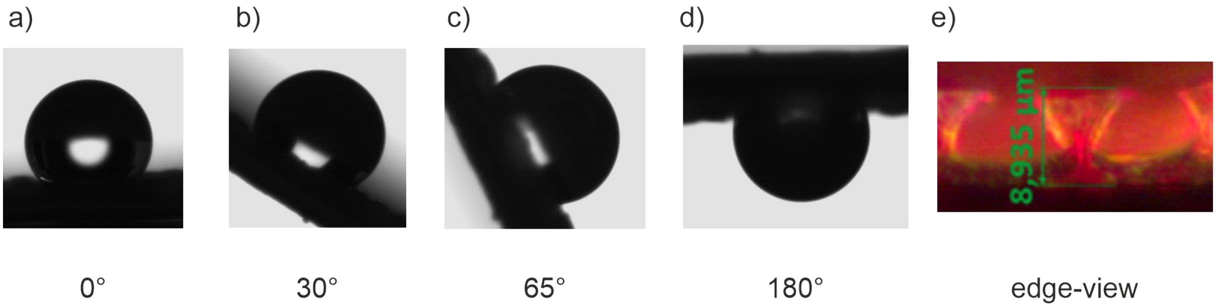

Figure S3: a) A water-droplet on a level irradiated coating. b) A water droplet hanging onto a caoting tilted by 30°, c) by 65° and d) by 180°. e) An edge-view of a coating showing the single layer of pores.

Section S9: Calibration of the Scratch Balance

The Fischertechnik 'ROBO TX Automation Robots' modelling kit comprising the scratch balance was arranged so that the tip of the needle, with a diameter of 87 µm (Figure S4), was placed on a fine balance (Kern Model PLJ 420-3F) at a fixed position. The needle was ensured to be at the same angle in this arrangement as in subsequent measurements for 'critical downward force' determination. The incremental addition of tin granules into the weighing boat was correlated to their corresponding output on the balance (Figure S5). The apparatus was covered with a plastic box during this calibration to minimise interference by airflow.

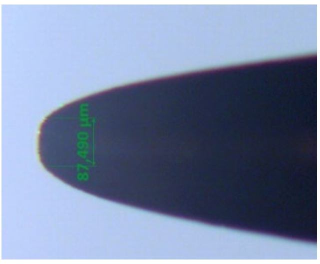

Figure S4: A micrograph of the needle used in the scratch balance.

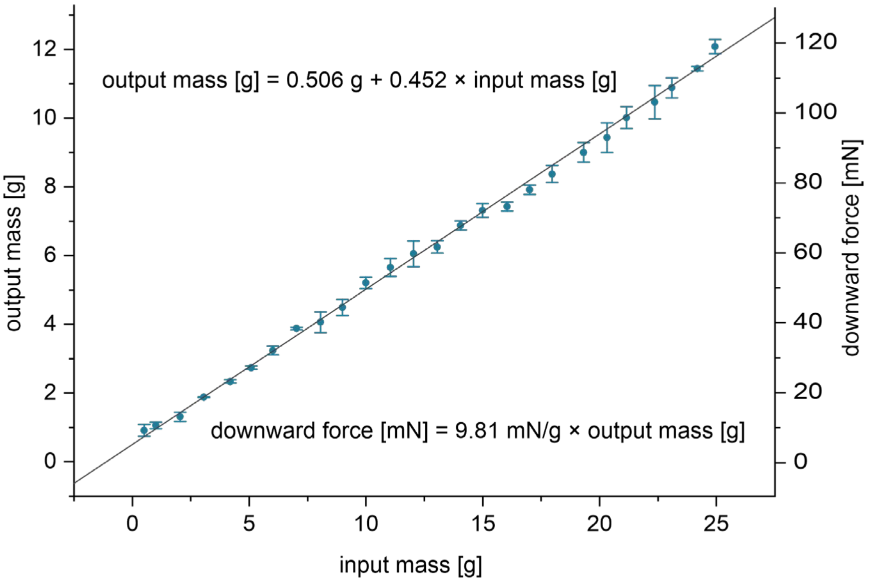

Figure S5: Calibration curve of the scratch balance, relating the input mass to the resulting downward force.

Section S10: Stability measurements

Section S10.1 relative stability measurement by the sand-flushing method

The relative mechanical stability of coatings obtained by dropcasting sols from Et_2O, $CHCl_3$ (irradiated and non-irradiated) and $PhCF_3$ was examined by flushing with sand (Figure S7). The setup consists of a glass funnel with a glass rod blocking the outflow tube from above. The funnel is filled with 250 g of dust free sea sand and the funnel is suspended above a holder for the glass slides. The holder is a wooden surface tilted by 45° on which the glass slides are held by staples. When the glass rod is lifted, the sand runs out of the funnel and onto the surface in 20 ± 1s.

The results were analysed by photography (before and after flushing) and analysis by imageJ (Figure S6). The relative proportion of removed coating is obtained by subtraction of the images and pixel counting (using the plugin Color Pixel Counter only comparing the cyan channel in each case) of the resulting difference-image. The results are presented in Table S1. Irradiated coatings from Et_2O were eroded by 20%, whereas coatings from $CHCl_3$ were eroded by 8% and coatings from $PhCF_3$ were eroded by only 1%. Despite the high mechanical stability of the $PhCF_3$-coatings, their omniphobicity was inferior due to the missing surface roughness. In contrast to that, the $CHCl_3$-coatings display both a high degree of roughness and stability and were thus investigated more thoroughly.

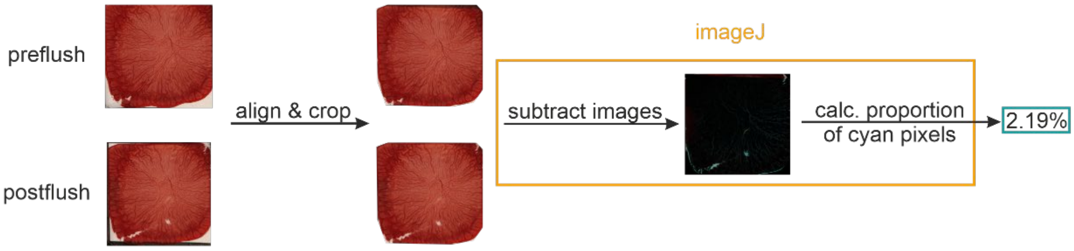

Figure S6: Image processing used for the analysis and calculation of material loss after sand abrasion.

Table S1: relative stability test by sand flushing, analysed by pixel count of cyan pixels in difference image of before and after flush.

solvent	before flush	after flush	difference
Et_2O			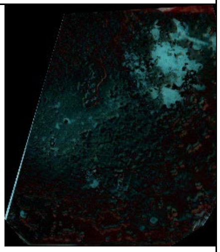 − 20%
$CHCl_3$		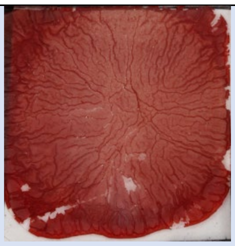	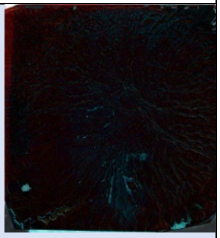 − 8%
$PhCF_3$			 − 1%

Figure S7: Setup for sand abrasion.

Section S10.2 stability measurements using the scratch balance

The Fischertechnik 'ROBO TX Automation Robots' modelling kit was arranged with 103 mm distance between the centre of the two rolls of the pulley system each with a diameter of 56 mm. A distance of 72 mm separated the top of the paper weighing boat and the roll seen on the left of Figure 4a (main text), while a 173 mm distance was measured from the centre of the other roll to the pivot point of the needle (Figure S4).

Using the ROBO pro software and a 9V/1.0W XS motor, constant speed of 2.5 mm/s for the 'car' carrying the sample under the needle was ensured. The needle was held at an angle 65° to the surface. In total, three scratches that fulfilled the threshold criterion (section 2.2.4.1) were applied to a single surface to ensure consistency across a single coating and the measurements repeated on two additional coatings, prepared under the same conditions, to calculate a mean critical mass. Surface scratches were analysed under the optical Zeiss microscope Axio Scope.A1 MAT and panoramas examined using ImageJ software. Using 0.1 g intervals, the weight required to remove over 90% of the material within the scratch and the mass 0.1 g lower than this critical value was determined.

References

S1 J.-S. Poh, S. Makai, T. von Keutz, D. N. Tran, C. Battilocchio, P. Pasau and S. V. Ley, Rapid Asymmetric Synthesis of Disubstituted Allenes by Coupling of Flow-Generated Diazo Compounds and Propargylated Amines, *Angew. Chem. Int. Ed.*, 2017, **56**, 1864–1868.

S2 D. Crich, K. Ranganathan and X. Huang, Generation and reaction of alkene radical cations under nonoxidizing conditions: synthesis of the pyrrolizidine nucleus, *Org. Lett.*, 2001, **3**, 1917–1919.

S3 C. Glaser, Beiträge zur Kenntniss des Acetenylbenzols, *Ber. Dtsch. Chem. Ges.*, 1869, **2**, 422–424.

S4 P. Siemsen, R. C. Livingston and F. Diederich, Acetylenic Coupling: A Powerful Tool in Molecular Construction, *Angew. Chem. Int. Ed.*, 2000, **39**, 2632–2657.

S5 P. Lucas, M. A. Jouani, H. Trabelsi and A. Cambon, Nouveaux procédés de préparation des isocyanates F-alkylés linéaires ou ramifiés à partir des iodures de 2-F-alkyléthyle, *J. Fluor. Chem.*, 1998, **92**, 17–22.

S6 N. Mureau, F. Guittard and S. Géribaldi, Convenient synthesis of thiols and disulfides in the polyfluorinated series incorporating a butylic spacer, *Tetrahedron Lett.*, 2000, **41**, 2885–2889.

S7 A. Wexler and S. Hasegawa, Relative humidity-temperature relationships of some saturated salt solutions in the temperature range 0 °C to 50 °C, *J. Res. Nat. Bur. Stand.*, 1954, **53**, 19–26.